EFFECT OF GEOMETRY AND SURFACE DISTRIBUTION OF HOLES ON SOUND AND LIGHT ABSORPTION PROPERTIES OF 3D-PRINTED PETG MATERIALS

MARTIN NEVRELA[1], MARTIN VASINA[2,3], PAVEL HRBACEK[3,4], VLADIMIR DEKYS[5]

[1]Centre for Advanced Innovation Technologies,
Faculty of Materials Science and technology,
VSB-Technical University of Ostrava, Czech Republic

[2]Department of Hydromechanics and Hydraulic Equipment,
Faculty of Mechanical Engineering,
VSB-Technical University of Ostrava, Czech Republic

[3]Department of Physics and Materials Engineering,
Faculty of Technology,
Tomas Bata University in Zlin, Czech Republic

[4]DT - Slovenska vyhybkaren, s.r.o.,
Nove Mesto and Vahom, Slovakia

[5]Department of Applied Mechanics,
Faculty of Mechanical Engineering,
University of Zilina, Slovakia

Noise and lighting are significant factors that have an impact on our health, environment, production quality, etc. The purpose of this paper is to investigate sound and light absorption properties of 3D-printed polyethylene terephthalate glycol (PETG) material specimens that were manufactured with two types of holes, namely with circular and square-shaped holes. In addition, the holes were printed with different dimensions, depths, shapes, and surface spacings. Different factors influencing the material´s ability to absorb sound and light were evaluated in this paper. It was found in this study that the type of holes, their spacing and depth have a big influence on sound and light absorption properties of the investigated samples compared to the smooth PETG material.

KEYWORDS

sound, light, absorption, hole geometry, spacing, depth

1 INTRODUCTION

The interaction between man and environment is continuous and in many cases hostile. Humans introduce many elements into the environment that either pollute it or alter its conditions with consequent negative effects on human health [Boffetta 2003], psyche, work safety, manufacturing productivity and quality [Lundstrom 2002, Sawacha 1999, Dawal 2006], etc. There are numerous factors influencing our environment. These include air, water, oil and plastic pollution, noise, lighting, mechanical vibration, temperature conditions, humidity, ionizing radiation, electromagnetic waves [Parsons 2020, Realyvasquez-Vargas 2020, Richard 2021, Strambersky 2021, Shuyushbayeva 2022], etc. Therefore, it is necessary to take

various measures to improve human comfort in practice [Yan 2022].

As mentioned above, noise and light are important environmental factors affecting human comfort in many areas of our lives, such as work, transportation, school and living spaces, etc. Noise is phenomenon that affects everybody and is generally defined as an unwanted sound or set of sounds [Muzet 2007]. It is necessary to eliminate undesirable noise by appropriate measures in practice. Similarly, it is necessary to create light comfort for humans. Visible light is a very important factor for the existence of life on Earth. Lighting conditions should be sufficient for performing the relevant activity. On the other hand, unwanted glare should be eliminated. The visible light is electromagnetic radiation with wavelengths in the range from 380 to 780 nm and photon energies from 1.6 to 3.2 eV, which can be perceived by a human eye [Gudkov 2017].

The objective of this paper is to investigate the sound and light absorption properties of 3D-printed PETG material samples, which were produced with different numbers, shapes, and sizes of surface holes. This paper discusses various factors that affect sound and noise propagation when using the investigated 3D-printed material structures. In practice, these 3D-printed materials can be used as suspended ceilings or lightweight walls in order to improve people´s well-being in their various activities, such as in lecture rooms, cinemas and libraries. Based on this study, new types of 3D printed materials can be developed and optimized to improve lighting and acoustic conditions in different environments.

2 SOUND AND LIGHT ABSORPTION PROPERTIES OF MATERIALS

2.1 Sound absorption properties of materials

As acoustic waves propagate from a sound source to a material´s surface, the incident acoustic energy is either reflected or absorbed by the material [Fediuk 2021]. Sound absorption properties of materials are expressed by the sound absorption coefficient $\alpha\,[-]$ as follows:

$$\alpha = 1 - \frac{E_R}{E_I} = \frac{E_A}{E_I} \tag{1}$$

Where:
E_R – reflected acoustic energy [J],
E_I – incident acoustic energy [J],
E_A – absorbed acoustic energy [J].

In general, better sound insulation properties of materials are obtained at higher values of the sound absorption coefficient α. Its value is affected by many factors, namely by material type, its thickness, structure, density, surface shape, excitation frequency and incidence angle of acoustic wave [Li 2022, Samsudin 2016].

2.2 Light absorption properties of materials

In the case of non-transparent solid materials, the incident luminous flux can either be reflected or absorbed when light propagates to a material surface [Makino 2010]. Light absorption properties of materials are characterized by the absorptance $A\,[-]$ as follows [Sliney 2007]:

$$A = \frac{\Phi_A}{\Phi_I} \tag{2}$$

Where:
Φ_A – absorbed luminous flux [lm],
Φ_I – incident luminous flux [lm].

A better ability to absorb light is generally obtained at higher values of the absorptance A. In the case of non-transparent materials, the absorptance is influenced mainly by surface color,

light wavelength, light incidence angle, surface roughness and shape [Brodersen 2007, Samsudin 2016].

3 MATERIALS

3.1 Materials

Specimens for the experimental measurements were produced from an PETG (polyethylene terephthalate glycol) material (Smart Materials 3D, Alcala la Real, Spain), which is one of the commonly used materials in 3D printing technique. It is a tough material, suitable for objects subjected to mechanical stress, hard, flexible, and resistant [Guerrero 2022]. The material for 3D printing was prepared in the form of a long filament with a diameter of 1.75 mm wound on a spool and was used to produce samples in order to evaluate their sound and light absorption properties.

3.2 Samples production

The investigated samples were designed using SolidWorks 2015 CAD software. Subsequently, they were printed using Creality CR-5 PRO printer (Shenzhen Creality 3D Technology Co., Ltd., Shenzhen, China) based on the FDM (Fused Deposition modelling) technique. The printing process was carried out at a temperature of approximately 235 °C and a printing speed of 50 mm/s.

All samples for the evaluation of sound absorption properties were made in the shape of a cylinder with a diameter of $d = 29$ mm and a thickness of $t = 4$ mm. They were produced with two types of holes, namely with circular and square holes (see Figures 1 and 2). Furthermore, the holes were produced with different characteristic sizes d or a (i.e., 1.5 and 3 mm), depths h (i.e., 1.5 and 3 mm), spacings p (i.e., 6 and 12 mm) and shapes. Various hole shapes of the investigated 3D-printed specimens are shown in Figure 3.
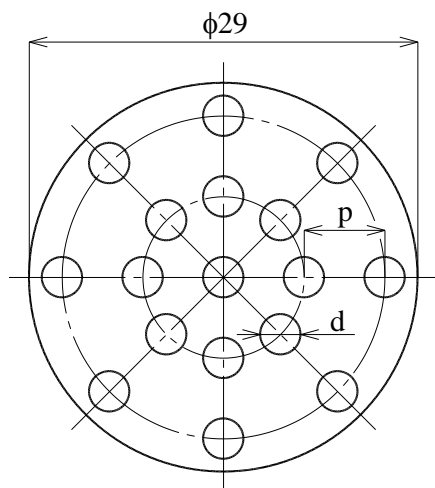

Figure 1. Specimen dimensions with circular holes for experimental measurements of sound absorption properties.
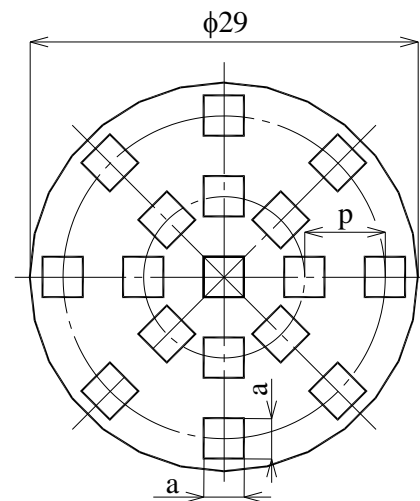

Figure 2. Specimen dimensions with square holes for experimental measurements of sound absorption properties.
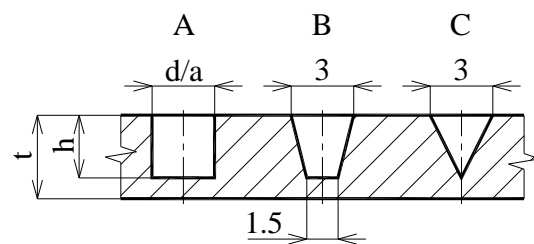

Figure 3. Investigated hole shapes (their cuts): A – cylinder/square prism, B - truncated cone/truncated square pyramid, C – cone/square pyramid.

In the case of the evaluation of light properties absorption properties, square plates with a thickness of $t = 4$ mm and a side of 225 mm were produced using 3D printing technology. Similarly, as in the case of the sound absorption properties, the plates were fitted with the same types (i.e., circular and square) of holes on their surface, as is shown in Figures 4 and 5. The characteristic parameters (i.e., d, a, h and p) and shapes of the holes were also the same (see Figures 1−3) as in the case sound absorption measurements of the investigated 3D-printed samples.
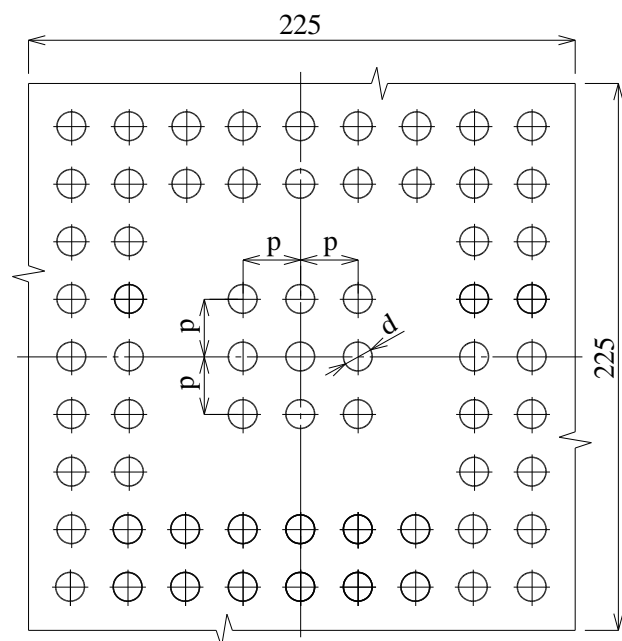

Figure 4. Specimen dimensions with circular holes for experimental measurements of light absorption properties.
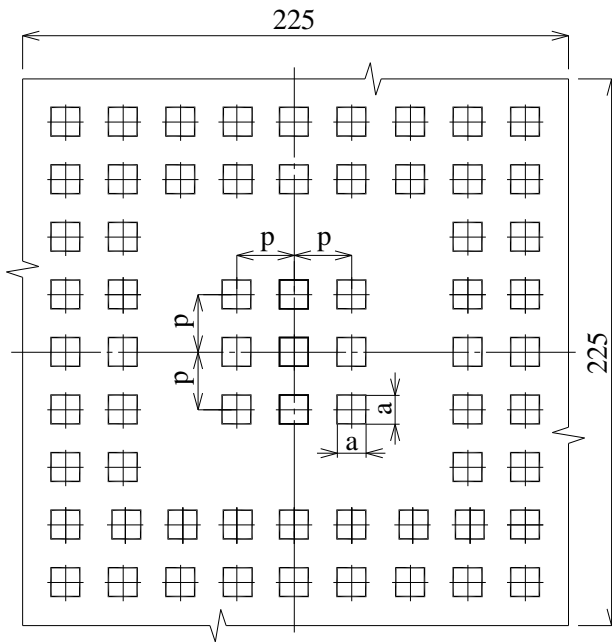
225

Figure 5. Specimen dimensions with square holes for experimental measurements of light absorption properties.

4 MEASUREMENT METHODOLOGY

4.1 Sound absorption coefficient

Frequency dependencies of the sound absorption coefficient of the studied 3D-printed PETG materials were measured by means of a two-microphone acoustic impedance tube (BK 4206) in combination with a signal PULSE multi-analyzer (BK 3560-B-030) and a power amplifier (BK 2706) in the frequency range of 200–6400 Hz (Brüel & Kjær, Nærum, Denmark), as is shown in Figure 6. In this case, acoustic waves (AW) are incident perpendicularly from the sound source (S) on the tested material specimen (M). All experiments were carried out at the ambient temperature of 20 °C.
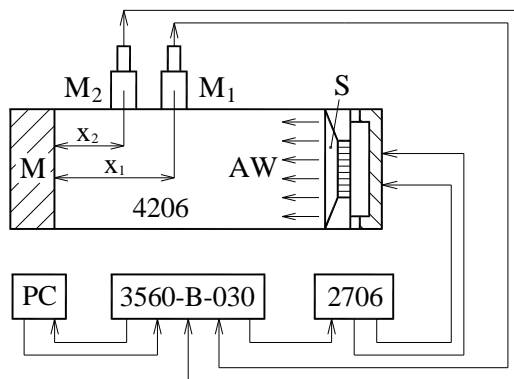

Figure 6. Schematic diagram of the experimental equipment for measuring frequency dependencies of the sound absorption coefficient

Experimental measurements of the sound absorption coefficient were performed by the transfer function method [ISO 10534-2 1998] that is based on the partial standing wave principle. In this case, the normal incidence sound absorption coefficient α is expressed as follows [Han 2003]:

$$\alpha = 1 - |r|^2 = 1 - r_r^2 - r_i^2 \tag{3}$$

Where:
r – normal incidence reflection factor [–],
r_r – real component of the factor r [–],

r_i – imaginary component of the factor r [–].
The normal incidence reflection factor is defined by the equation:

$$r = \frac{H_{12} - H_I}{H_R - H_{12}} \cdot e^{2k_0 \cdot x_1 i} \tag{4}$$

Where:
H_{12} – complex acoustic transfer function [–],
H_I – transfer function of incident wave [–],
H_R – transfer function of reflection wave [–],
k_0 – wave number [m^{-1}],
x_1 – distance (see Figure 6) between the tested material sample and the microphone M$_1$ [m],
i – imaginary unit.
The above-mentioned transfer functions are expressed by the equations:

$$H_{12} = \frac{p_2}{p_1} = \frac{e^{k_0 \cdot x_2 i} + r \cdot e^{-k_0 \cdot x_2 i}}{e^{k_0 \cdot x_1 i} + r \cdot e^{-k_0 \cdot x_1 i}} \tag{5}$$

$$H_I = e^{-k_0 \cdot (x_1 - x_2)i} \tag{6}$$

$$H_R = e^{k_0 \cdot (x_1 - x_2)i} \tag{7}$$

Where:
p_1 – complex acoustic pressure measured by the microphone M$_1$ [Pa],
p_2 – complex acoustic pressure measured by the microphone M$_2$ [Pa],
x_2 – distance (see Figure 6) between the tested material sample and the microphone M$_2$ [m].

4.2 Light absorptance

Light absorption properties, (i.e., the absorptance A) of the studied 3D-printed PETG specimens were investigated according to [CSN EN ISO 360001-1 2006] standard based on the reflectance R [–], which was determined based on the illumination ratio:

$$R = \frac{E_r}{E_i} \tag{8}$$

Where:
E_r – reflected illuminance from the tested material sample [lx],
E_i – incident illuminance on the material sample under test [lx].
The above-mentioned illuminances were measured using the digital illuminometer Voltcraft MS-1300 (Voltcraft, Hirschau, Germany) under diffuse daylight (i.e., without artificial lighting sources). Experimental measurements of both illuminances for each sample surface were performed twenty times. The light absorptance A was subsequently determined from the formula:

$$A = 1 - R \tag{9}$$

Finally, average values and standard deviations of the absorptance were evaluated for each of the 3D-printed samples examined.

5 RESULTS AND DISCUSSION

5.1 Sound absorption properties

Different factors that have an influence on sound absorption properties of the investigated 3D-printed samples are evaluated in the following subchapters.

5.1.1 Effect of hole type

As stated above, the tested specimens with two types of holes, namely with the circular (C) and square (S) hole cross-sections, were manufactured using 3D printing technology. The effect of

the hole type (in this case in the shape of the cylinder or square prism shapes) on sound absorption behavior of the tested samples is shown in Figures 7 and 8.

Figure 7 shows the frequency dependencies of the sound absorption coefficient of the specimens, which were made with a minimum number of circular holes (i.e., p = 12 mm) and minimum hole dimensions (i.e., a = d = h = 1.5 mm). In addition, the frequency dependencies of the sound absorption coefficient of these samples are compared with the full (F) 3D-printed PETG specimen (i.e., without surface holes). It is evident that the sample containing square holes showed a better ability to attenuate noise over a substantial part of the frequency range (i.e., from 1.5 to 4.5 kHz). It is caused by a higher surface of holes in the shape of the square prism (see Figure 3, A-type holes) compared to the cylinder shapes, which leads to higher internal friction during the propagation of acoustic waves inside the square holes. On the contrary, the sample containing circular holes exhibited better sound absorption properties at higher excitation frequencies (i.e., from 5 to 6 kHz) compared to the sample manufactured with square holes. Sound damping properties of both samples were practically the same at low excitation frequencies (i.e., at f < 1.5 kHz). It was also found that the full smooth sample is generally characterized by worse sound absorption properties compared the samples manufactured with both types of holes. Therefore, shape material surfaces generally lead to a higher dissipation of acoustic energy into heat during the propagation of incident acoustic waves on the material surfaces under investigation.
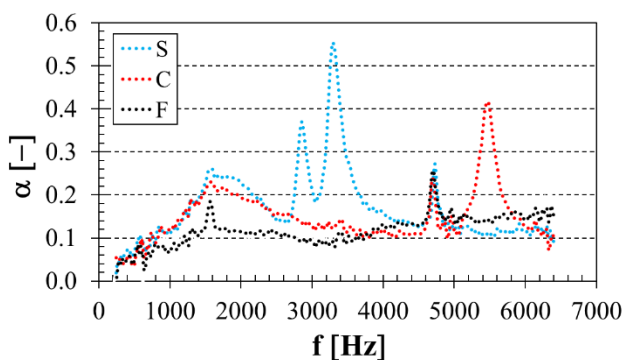

Figure 7. Effect of the hole type on the frequency dependencies of the sound absorption coefficient for specimens with holes of the following parameters: a = 1.5 mm, d = 1.5 mm, h = 1.5 mm, p = 12 mm.

The frequency dependencies of the sound absorption coefficient of the samples, which were made with a maximum number of circular holes (i.e., p = 6 mm) and maximum hole dimensions (i.e., a = d = h = 3 mm), are compared with sound absorption properties of the full (F) sample in Figure 8. Again, the samples produced with both types of holes exhibited better sound damping properties over a substantial part of the measured frequency range. Similarly, as in the previous case (see Figure 7), sound absorption properties of the tested samples are not affected by the hole type at low excitation frequencies (i.e., at f < 1.5 kHz). The sample containing circular holes again showed better sound absorption properties at higher excitation frequencies (i.e., at f > 3.5 kHz). In the middle frequency band (i.e., from 1.5 to 3.5 kHz), the hole type on the sample ability to damp sound is not entirely clear. It is strongly influenced by the excitation frequency (see Figure 8).

Based on experimental measurements, it can be concluded that the hole type has a significant effect on sound absorption properties of the tested 3D-printed specimens only at higher excitation frequencies, mainly in the frequency range from 1.5 to 4.5 kHz. At low excitation frequencies, the effect of the hole type on sound absorption was negligible.
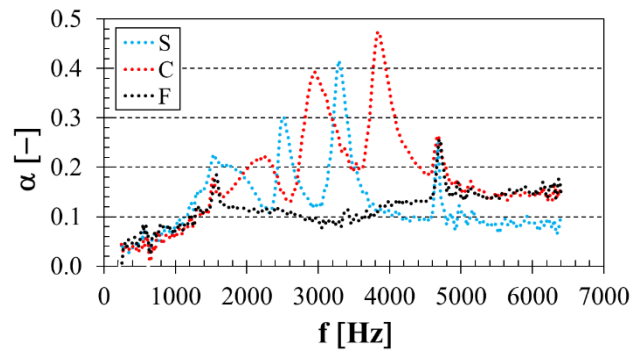

Figure 8. Effect of the hole type on the frequency dependencies of the sound absorption coefficient for specimens with holes of the following parameters: a = 3 mm, d = 3 mm, h = 3 mm, p = 6 mm.

5.1.2 Effect of hole size

As is shown in Figures 9 and 10, the hole sizes (i.e., the cross-section size of circular or square holes) has a significant effect on sound absorption performance of the tested 3D-printed specimens. It is evident that a higher sound damping ability was found for specimens containing holes of larger dimensions that are characterized by higher internal friction during the propagation of acoustic waves inside these holes. This was due to the larger internal surfaces of the holes, which is subsequently accompanied by greater friction and thus also the transformation of the incident acoustic energy into heat.
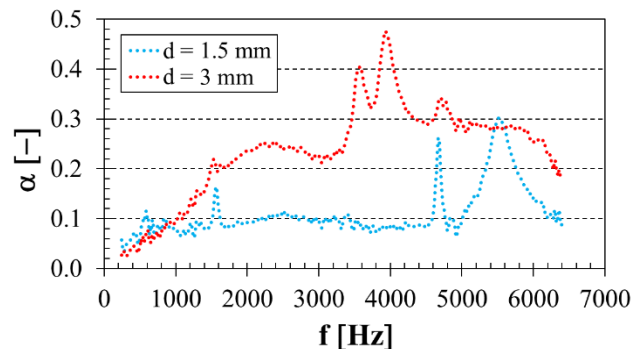

Figure 9. Effect of the hole size on the frequency dependencies of the sound absorption coefficient for specimens with circular holes of the following parameters: h = 1.5 mm, p = 6 mm.
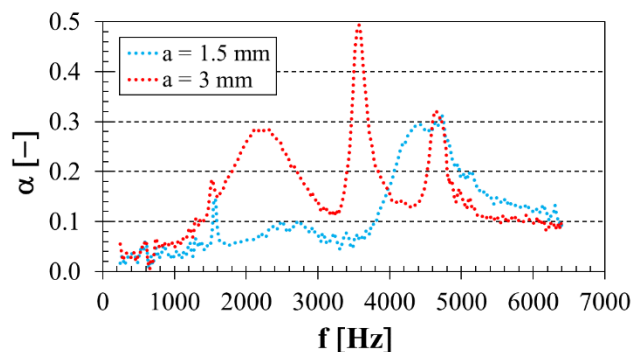

Figure 10. Effect of the hole size on the frequency dependencies of the sound absorption coefficient for specimens with square holes of the following parameters: h = 3 mm, p = 12 mm.

5.1.3 Effect of hole spacing

The effect of the spacing between holes is shown in Figure 11. In this case, the investigated samples were made with square holes of side length a = 1.5 mm and depth h = 3 mm. It is obvious that a smaller spacing between the square holes led to a better ability to damp incident acoustic waves over a substantial part of the frequency range. Therefore, a higher number of holes on the

sample surface results in lower sound reflection from the material surface, which is accompanied by a higher dissipation of incident acoustic energy into heat.
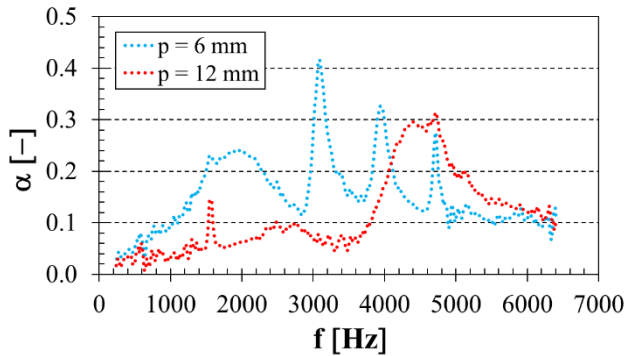

Figure 11. Effect of the hole spacing on the frequency dependencies of the sound absorption coefficient for specimens with square holes of the following parameters: $a = 1.5$ mm, $h = 3$ mm.

5.1.4 Effect of hole depth

The influence of the hole depth for specimens manufactured with circular holes of diameter $d = 1.5$ mm and spacing $p = 12$ mm is demonstrated in Figure 12. It is evident that sound absorption properties of the tested samples increased with increasing the hole depth in a substantial part of the measured frequency range. This is due to the fact that a higher hole depth corresponds to higher inner surfaces of the holes. It is accompanied by higher internal friction during the propagation of acoustic waves inside the holes and, consequently, by a higher dissipation of incident acoustic energy into heat.
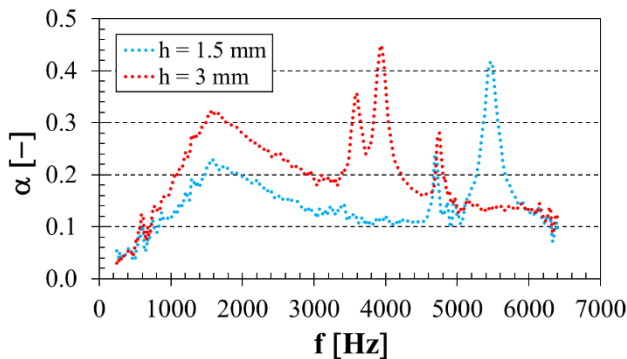

Figure 12. Effect of the hole depth on the frequency dependencies of the sound absorption coefficient for specimens with circular holes of the following parameters: $d = 1.5$ mm, $p = 12$ mm.

5.1.5 Effect of hole shape

In previous cases (see Figures 7-12), the frequency dependencies of the sound absorption coefficient are shown for A-type holes, i.e., in the shape of a cylinder and a square prism. In addition (see Figure 3), 3D-printed specimens were also produced with chamfered holes in the shape of truncated cone/truncated square pyramid (i.e., B-type holes) and cone/square pyramid (i.e., C-type holes). Examples of the effect of the hole shape on sound absorption of the investigated PETG samples with circular and square holes with the given parameters (i.e., dimensions d or a, p and h) are shown in Figures 13 and 14. It is evident that the hole shape has a significant influence on sound absorption properties, mainly at higher excitation frequencies (i.e., at $f > 1.5$ kHz). At low excitation frequencies (i.e., at $f < 1.5$ kHz), the effect of the hole type on sound absorption was negligible.
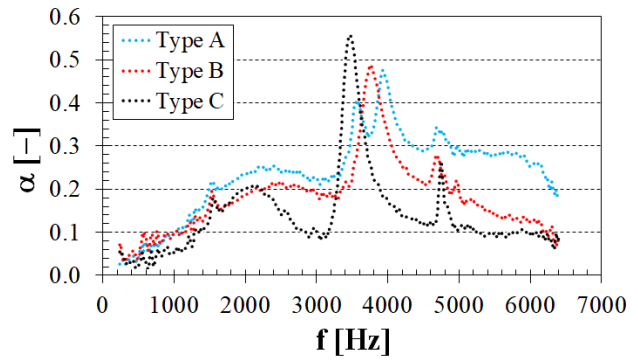

Figure 13. Effect of the hole shape on the frequency dependencies of the sound absorption coefficient for specimens with circular holes of the following parameters: $d = 3$ mm, $p = 6$ mm, $h = 1.5$ mm.
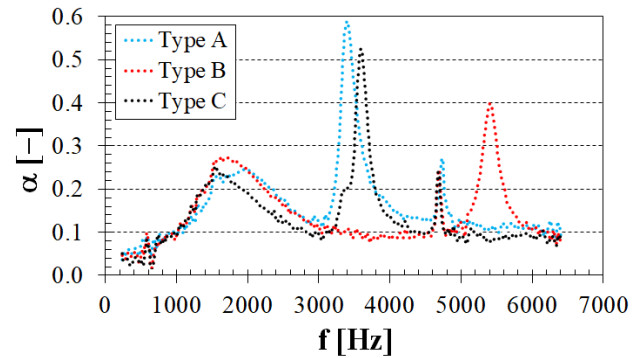

Figure 14. Effect of the hole shape on the frequency dependencies of the sound absorption coefficient for specimens with square holes of the following parameters: $a = 3$ mm, $p = 12$ mm, $h = 1.5$ mm.

5.1.6 Effect of excitation frequency

As shown above in Figures 7-14, sound absorption properties of the studied 3D-printed PETG specimens containing square or circular holes are strongly influenced by the excitation frequency f. It is obvious that a relatively low sound absorption ability was found at low excitation frequencies, namely at $f < 1$ kHz. Contrarily, in some cases, the highest sound absorption properties (i.e., $\alpha_{max} \cong 0.6$) were obtained in the frequency range from 3.3 to 3.8 kHz. It can also be seen from Figures 7-14 that the sound absorption peaks are observed at certain excitation frequencies depending on the sample type. In this case, acoustic energy is reduced due to air compressibility and air movement in the holes that creates friction with the walls of holes. As a result, the acoustic energy is converted into heat and subsequently dissipated.

5.2 Light absorption properties

Various factors affecting the light absorptance A of the investigated 3D-printed samples are summarized and compared with the full 3D-printed PETG specimen (F) in Tables 1 and 2.

It is obvious, similar to the sound absorption behaviour, that the lowest light absorption properties (or the minimum absorptance $A_{min} = 0.505$) were found for the smooth PETG material specimen (i.e., without surface holes). On the contrary, the maximum absorptance $A_{max} = 0.552$ was for the 3D-printed PETG sample that was made with a maximum number of square holes (i.e., $p = 6$ mm) and maximum hole dimensions (i.e., $a = h = 3$ mm). Therefore, the specimens containing holes are characterized by a higher ability to absorb light compared to the full 3D-printed PETG specimen (F). It is caused by multiple light reflections as light propagated inside the holes and accompanied by a higher transformation of the incident light energy into heat. As in the case of sound absorption properties, the light absorptance (see

Tables 1 and 2) generally increased with increasing the number of surface holes (i.e., p = 6 mm) and their dimensions (i.e., $a = d = h$ = 3 mm). Other factors, such as the shape (i.e., square or circular) and type (i.e., type A, B or C) of holes, were negligible in terms of light absorption.

Shape type	d [mm]	p [mm]	h [mm]	A [−]
A	1.5	6	1.5	0.535 ± 0.013
			3.0	0.540 ± 0.017
		12	1.5	0.524 ± 0.009
			3.0	0.527 ± 0.012
	3.0	6	1.5	0.547 ± 0.025
			3.0	0.549 ± 0.016
		12	1.5	0.534 ± 0.011
			3.0	0.536 ± 0.018
B	3.0	6	1.5	0.541 ± 0.023
			3.0	0.547 ± 0.019
		12	1.5	0.536 ± 0.020
			3.0	0.540 ± 0.015
C	3.0	6	1.5	0.541 ± 0.017
			3.0	0.543 ± 0.012
		12	1.5	0.536 ± 0.015
			3.0	0.539 ± 0.018
F	−	−	−	0.505 ± 0.019

Table 1. Measured values of the light absorptance A of the 3D-printed specimens with circular holes.

Shape type	a [mm]	p [mm]	h [mm]	A [−]
A	1.5	6	1.5	0.540 ± 0.017
			3.0	0.542 ± 0.013
		12	1.5	0.532 ± 0.012
			3.0	0.537 ± 0.019
	3.0	6	1.5	0.545 ± 0.020
			3.0	0.552 ± 0.024
		12	1.5	0.538 ± 0.018
			3.0	0.540 ± 0.023
B	3.0	6	1.5	0.541 ± 0.016
			3.0	0.550 ± 0.027
		12	1.5	0.532 ± 0.018
			3.0	0.540 ± 0.017
C	3.0	6	1.5	0.536 ± 0.026
			3.0	0.544 ± 0.017
		12	1.5	0.530 ± 0.025
			3.0	0.533 ± 0.021
F	−	−	−	0.505 ± 0.019

Table 2. Measured values of the light absorptance A of the 3D-printed specimens with square holes.

6 CONCLUSIONS

The aim of this paper was to investigate the influence of the geometry and surface distribution of holes on sound and light absorption properties of 3D-printed PETG materials. It can be concluded that the geometry and number of surface holes on the investigated material samples has a significant influence on their sound and light absorption. It was found in this study that better sound and light absorption properties were generally found for 3D-printed PETG specimens containing a higher number of surface holes with larger dimensions. In these cases, the sound or light propagation through the holes was

characterized by a higher internal friction of sound or light waves in these material structures. It was subsequently accompanied by a higher dissipation of the acoustic or light energy into heat compared to the smooth specimen, which was manufactured without surface holes.

3D printing is a developing and perspective technology that finds application in many areas of our lives. It allows the production of lightweight materials of various shapes and structures compared to conventional manufacturing technologies, which leads to time, material, and energy savings. For these reasons, it is also possible to develop advanced 3D-printed lightweight material structures to absorb unwanted noise and light in practice, which can lead to improved human comfort. For example, during presentations in lecture halls and rooms, film projections in cinemas, etc. Furthermore, new developed 3D-printed materials can also have an aesthetic function in closed rooms.

REFERENCES

[Boffetta 2003] Boffetta, P. and Nyberg, F. Contribution of environmental factors to cancer risk. British Medical Bulletin, 2003, Vol.68, pp 71-94. ISSN 0007-1420

[Lundstrom 2002]Ondstrom, T., et al. Organizational and environmental factors that affect worker health and safety and patient outcomes. American Journal of Infection Control, April 2002, Vol.30, No.2., pp 93-106. ISSN 0196-6553

[Sawacha 1999] Sawacha, E., et al. Factors affecting safety performance on construction sites. International Journal of Project Management, October 1999, Vol.17, No.5., pp 309-315. ISSN 0362-7863

[Dawal 2006] Dawal, S. Z. M. and Taha, Z. The effect of job and environmental factors on job satisfaction in automotive industries. International Journal of Occupational Safety and Agronomics, 2006, Vol.12, No.3, pp 267-280. ISSN 1080-3548

[Parsons 2000] Parsons, K. C. Environmental ergonomics: a review of principles, methods and models. Applied Ergonomics, December 2000, Vol.31, No.6, pp 581-594. ISSN 0003-6870

[Realyvasquez-Vargas 2020] Realyvasquez-Vargas, A., et al. The Impact of Environmental Factors on Academic Performance of University Students Taking Online Classes during the COVID-19 Pandemic in Mexico. Sustainability, November 2020, Vol.12, No.21, 9194. ISSN 2071-1050

[Richard 2021] Richard, F. J., et al. Warning of nine pollutants and their effects on avian communities. Global Ecology and Conservation, December 2021, Vol.32, e01898. ISSN 2351-9894

[Strambersky 2021] Strambersky, R., et al. Cogeneration Unit Noise Reduction by its Case. MM Science Journal, June 2021, Vol.2021, pp 4501-4504. ISSN 1803-1269

[Shuyushbayeva 2022] Shuyushbayeva, N., et al. Opportunities of ecologization of physics course. Bulgarian Chemical Communications, 2022, Vol.54, pp 77-80. ISSN 0861-9808

[Yan 2022] Yan, Y. C. and Jia, Y. Y. A Review of Human Comfort Factors, Measurements, and Improvement in Human-Robot Collaboration. Sensors, October 2022, Vol.22, No.19, 7431. ISSN 1424-8220

[Gudkov 2017] Gudkov, S. V., et al. Effect of Visible Light on Biological Objects: Physiological and Pathophysiological Aspects. Physics of Wave Phenomena, July 2017, Vol.25, No.3, pp 207-213. ISSN 1541-308X

[Fediuk 2021] Fediuk, R., et al. Acoustic Properties of Innovative Concretes: A Review. Materials, January 2021, Vol.14, No.2, 398. ISSN 1996-1944

[Li 2022] Li, X., et al. Research Progress on Sound Absorption of Electrospun Fibrous Composite Materials. Nanomaterials, April 2022, Vol.12, No.7, 1123. ISSN 2079-4991

[Samsudin 2016] Samsudin, E. M., et al. A Review on Physical Factors Influencing Absorption Performance of Fibrous Sound Absorption Material from Natural Fibers. ARPN Journal of Engineering and Applied Sciences, March 2016, Vol.11, No.6, pp 3703-3711. ISSN 1819-6608

[Makino 2010] Makino, T. and Wakabayashi, H. A new Spectrophotometer System for Measuring Hemispherical Reflectance and Normal Emittance of Real Surfaces Simultaneously. International Journal of Thermophysics, December 2010, Vol.31, No.11-12, pp 2283-2294. ISSN 0195-928X

[Sliney 2007] Sliney, D. H. Radiometric quantities and units used in photobiology and photochemistry: Recommendations of the Commission Internationale de l´Eclairage (International Commission on Illumination). Photochemistry and Photobiology, March-April 2007, Vol.83, No.2, pp 425-432. ISSN 0031-8655

[Brodersen 2007] Brodersen, C. R. and Vogelmann, T. C. Do epidermal lens cells facilitate the absorptance of diffuse light. American Journal of Botany, July 2007, Vol.94, No.7, pp 1061-1066. ISSN 0002-9122

[Guerrero 2022] Guerrero, R., et al. Multidirectional traps as a new assessment system of soil wind erosion. Scientia Agricola, July 2022, Vol.72, No.4, e20200342. ISSN 1678-992X

[ISO10534-2 1998] Standard ISO 10534-2:1998. Acoustics-Determination of Sound Absorption Coefficient and Impedance in Impedance Tubes-Part 2: Transfer-Function Method.

[Han 2003] Han, F. S., et al. Acoustic absorption behaviour of an open-celled aluminum foam. Journal of Physics D: Applied Physics, February 2003, Vol.36, No.3, pp 294-302. ISSN 0022-3727

[CSN EN ISO 36001-1 2006] Standard CSN 360011-1:2006. Measurement of lighting in interior; Part 1: Basic provisions). Prague, Czech Office for Standards, Metrology and Testing.

CONTACTS:

Ing. Martin Nevrela
VSB - Technical University of Ostrava, Centre for Advanced Innovation Technologies,
17. listopadu 2172/15, CZ-708 00 Ostrava-Poruba
+420 597 324 384, martin.nevrela@vsb.cz

Assoc. Prof. Ing. Martin Vasina, Ph.D.
VSB - Technical University of Ostrava, Department of Hydromechanics and Hydraulic Equipment,
17. listopadu 2172/15, CZ-708 00 Ostrava-Poruba
+420 597 995 210, martin.vasina@vsb.cz

Ing. Pavel Hrbacek
Tomas Bata University in Zlin, Department of Physics and Materials Engineering,
Vavrečkova 5669, CZ-760 01 Zlin
+420 596 035 112, p_hrbacek@utb.cz

Assoc. Prof. Ing. Vladimir Dekys, CSc.
University of Zilina, Department of Applied Mechanics,
Univerzitna 8215/1, SK-010 26 Zilina
+421 41 5132954, vladimir.dekys@fstroj.uniza.sk